https://doi.org/10.17221/148/2024-PPS

Allelopathic potential of *Turnera subulata* leaf extract on choy sum (*Brassica chinensis* var. *parachinensis*) via untargeted metabolomics

Nor Atirah Mohd Aridi[1], *Nornasuha Yusoff*[1]*, *Muhd Arif Shaffiq Sahrir*[1], *Kamalrul Azlan Azizan*[2]

[1]*School of Agriculture Science and Biotechnology, Faculty of Bioresources and Food Industry, Universiti Sultan Zainal Abidin, Besut, Terengganu, Malaysia*
[2]*Metabolomics Research Laboratory, Institute of Systems Biology (INBIOSIS), Universiti Kebangsaan Malaysia, Bangi, Selangor, Malaysia*

**Corresponding author: nornasuhayusoff@unisza.edu.my*

Citation: Mohd Aridi N.A., Yusoff N., Sahrir M.A.S., Azizan K.A. (2026): Allelopathic potential of *Turnera subulata* leaf extract on choy sum (*Brassica chinensis* var. *parachinensis*) via untargeted metabolomics. Plant. Protect. Sci., 62: 79–92.

Abstract: Allelopathic plants release phytotoxic compounds that contribute to their invasiveness by suppressing nearby species. However, it remains unclear which exact mode of action (MOA) underlies the allelopathy. This study explores the allelopathic mechanisms of *Turnera subulata* on the recipient indicator plant choy sum using a metabolomics approach. Briefly, *T. subulata* leaf aqueous extracts (LAEs) at different concentrations (0.0, 0.1, 1.0, 10.0, 50.0, and 100.0 mg/mL) were sprayed at 100 mL/m^2 on choy sum seedlings at the two to three leaf stage. After 21 days, the Soil Plant Analysis Development (SPAD) values and photosynthetic pigments of the exposed choy sum were measured, and their metabolites were subjected to a gas chromatography-mass spectrometer (GC-MS) analysis. The results revealed a 25% decrease in the SPAD, a reduction of 65% (*chl a*) and 71% (*chl b*), and a 45% reduction in the stomatal length at 100 mg/mL. A total of 15 significant metabolites ($P < 0.05$) with variables important for the projection score exceeding 1 (VIP > 1) were selected as the important biomarkers. These metabolites were identified as amino acids, carbohydrates, and fatty acids. The findings reveal the allelopathic potential of *T. subulata* and provide insights into the response of choy sum in response to the allelopathic activity of *T. subulata* LAEs.

Keywords: allelopathy; aqueous extract; GC-MS analysis; metabolites; pathway analysis

Biotic and abiotic stresses pose significant challenges to crop production, reducing the annual crop yield (Oshunsanya et al. 2019). These stresses impact the enzyme activity, polynucleotides, and nutrient transport systems, which hinder plant growth and metabolism (Katiyar et al. 2022). To adapt to this stress, plants incorporate metabolomics, transcriptomics, proteomics, and genomes, either separately or in combination (Anzano et al. 2022). Specifically, analytical techniques like liquid chromatography-mass spectrometry (LC-MS), gas chromatography-mass spectrometry (GC-MS), or Fourier-transform infrared (FTIR) spectroscopy are used to study the metabolomics profile of plants under stress. These methods help to identify the phytochemicals that plants produce in response to various environmental stimuli (Wishart et al. 2022; Mashabela et al. 2023).

Supported by the Research Grant No. FRGS/1/2019/WAB01/UNISZA/03/2 from the Ministry of Higher Education, Malaysia.

https://doi.org/10.17221/148/2024-PPS

Allelopathy is the chemical interaction between plants, where one plant releases allelochemicals that can inhibit or stimulate the growth of nearby plants through leaching, root exudation, volatilisation, or residue decomposition. Allelopathic effects have been well-documented in *Jatropha gossypiifolia*, *Chrysopogon zizanioides* (L.) Roberty, and *Euphorbia jolkinii*, helping to elucidate the mode of action (MOA) of allelochemicals at the metabolic pathway level (de Almeida et al. 2024; Sahrir et al. 2024; Xiao et al. 2025). Metabolomics has identified allelochemicals and understanding stress-induced metabolic shifts. For instance, GC-MS-based metabolomic studies have elucidated the allelopathic responses in *Arabidopsis thaliana* exposed to *Ageratina adenophora*, and in *Lactuca sativa* treated with *Tagetes minuta* extracts, highlighting changes in the phenylpropanoid, amino acid, and sugar metabolism. These studies reinforce the significance of metabolomics in unravelling allelopathic MOA.

Turnera subulata is a medium-sized perennial shrub commonly called the white buttercup, sulfur alder, dark-eyed Turnera, and white alder under the Passifloraceae family (Henning et al. 2023). It is native to Central and South America, but has also naturalised in tropical and subtropical regions including Malaysia, where it often grows along roadsides, disturbed habitats, and in ornamental gardens (Saravanan et al. 2018; Andrade-Pinheiro et al. 2023). Traditionally, it has been used in folk medicine for its antibacterial, anti-inflammatory, and antioxidant properties (Chai & Wong 2012; Saravanan et al. 2018). This rich phytochemical profile is indicative of having high allelopathic potential, as many of these compounds have been associated with phytotoxic effects in previous allelopathy studies. Studies on the phytochemical composition of *T. subulata* have shown the presence of triterpenoids, fatty acids, alkaloids, tannins, cyanogenic glycosides, flavonols, and other phenolic compounds, all of which are linked to a variety of bioactive characteristics (Szewczyk et al. 2012; Brito Filho et al. 2014; Saravanan et al. 2020).

T. subulata was selected due to previous studies that proved its noteworthy allelopathic potential and the presence of secondary metabolites, often linked to allelopathic interactions (Saravanan et al. 2018; Luz et al. 2022). Furthermore, its availability, rapid growth, and ability to thrive in challenging environments make *T. subulata* a promising candidate for further study. However, the mode of actions (MOAs) by which *T. subulata* affects a target plant species are still largely unknown. *T. subulata* is known for its high antioxidant and phytochemical contents, but the majority of studies have focused on its medicinal uses rather than its allelopathic potential against a targeted plant at the metabolic level. Although a previous study (Yaakob et al. 2020) had suggested the allelopathic properties of *T. subulata*, the specific metabolic mechanisms through which *T. subulata* operates are still unclear and need further investigation.

This study examines the biochemical responses of choy sum to different concentrations of *T. subulata* leaf aqueous extract (LAE) using untargeted GC-MS metabolomics. Choy sum (*Brassica chinensis* var. *parachinensis*) was selected for its consistent growth, high germination rate, and short cultivation period of about 30 days (Zou et al. 2021). *Brassica* species are well-studied in allelopathy and metabolomics (Tashim et al. 2021; Zou et al. 2021; Huang et al. 2024) and serve as models in research due to their rich bioactive phytochemicals (Jahangir et al. 2009). This research aims to uncover the allelopathic effects of *T. subulata* by analysing the metabolite changes and metabolic pathways in the target plants, potentially identifying new allelochemicals influencing the plant metabolism. The output of this study can bridge the gap between phytochemical profiles and their biochemical effects on crops, enhancing our understanding of their mode of actions, which can support sustainable weed management and natural herbicide alternatives.

MATERIAL AND METHODS

Collection of *T. subulata*. The *T. subulata* was cultivated in a sandy loam soil in a polybag (16' X 16') at the UniSZA herbal garden (05°45'10.0" N, 102°37'41.9" E). A voucher specimen was deposited at the Herbarium of Universiti Sultan Zainal Abidin (Voucher No: UniSZA/A/000000043).

Aqueous extract preparation. After four months of planting, the leaves were collected and washed with tap water. Subsequently, the leaves were then dried in an oven at 60 °C for 24 h and finely ground by a microfine grinder (MF 10, IKA, Staufen, Germany). 100 mg of leaf powder were soaked in 100 mL distilled water for 72 h at 4 °C.

https://doi.org/10.17221/148/2024-PPS

The extract was filtered, and the resulting extract was diluted to concentrations of 0.1, 1.0, 10.0, 50.0, and 100.0 mg/mL with distilled water. The choy sum seeds utilised as the recipient indicator plant were purchased from Leckat Corporation Sdn. Bhd., Kuala Lumpur, Malaysia.

Pot bioassay experiment. Three choy sum seeds were planted in a pot (size: 15 cm height × 10 cm width), which was filled with 800 g of the sandy loam soil per pot (pH 7.7, organic C: 2.47%, sand: 67.90%, clay: 17.30%, silt: 14.80%). A garden sprayer was used to apply *T. subulata* LAE at different concentrations (0.1, 1.0, 10.0, 50.0, and 100.0 mg/mL) at a 100 mL/m^2 rate after the choy sum grew to two to three true leaves. Each pot was sprayed with a half-strength Hoagland solution (20 mL) two weeks after germination. The experiment was set up using a randomised complete block design (RCBD) with five replications in a greenhouse with a temperature of 30.3 °C ± 3.3 °C and a relative humidity of 66.82 ± 13.0%. Choy sum sprayed with distilled water was used as a control. The leaves of choy sum were collected on the 21st day after LAE application for the physiological measurement and metabolomics analysis.

Photosynthetic pigments. On the 21st day of the experiment, the Soil Plant Analysis Development (SPAD) of the choy sum leaves was measured with a portable SPAD meter (502 plus, Konica Minolta, Tokyo, Japan). The method addressed by Lichtenthaler and Wellburn (1983) was followed to measure the chlorophyll content (*chl a* and *chl b*). After 100 mg samples were extracted in 5 mL 80% acetone, the 663 nm and 645 nm absorbances were determined. The given equation was used to calculate the pigment concentrations:

$$\text{Chlorophyll } a \text{ (mg/mL)} = 12.7\,(A663) - 2.69\,(A645)$$

$$\text{Chlorophyll } b \text{ (mg/mL)} = 22.9\,(A645) - 4.68\,(A663)$$

Observation of stomata length. A scanning electron microscope (SEM) (JSm-636OLA, JEOL, Tokyo, Japan) was used to analyse the abaxial surface of the leaves in order to determine the effect of the *T. subulata* LAE on the stomatal length of the choy sum, following the method by Gowtham et al. (2016).

Preparation of extract for metabolite identification. The leaves of the choy sum were collected on the 21st day after the LAE application for a metabolomics analysis. Briefly, the samples were ground in liquid nitrogen. Then, about 20 mg of the sample were extracted with methanol/water (80/20 *v/v*) and then followed by chloroform/water (50/50 *v/v*). The extracts were subjected to sonication for 15 min, followed by centrifugation at 12 000 revolutions per minute for 20 min. The derivatisation process involved 50 µL of N,O-bis(trimethylsilyl)trifluoroacetamide (BSTFA) in pyridine. Subsequently, the samples were placed in a ThermoMixer C (Eppendorf, Germany) and subjected to incubation at a temperature of 60 °C for a duration of 1 h, after which they were injected into the GC-MS. For each sample, 20 µL of ribitol was added as an internal standard.

GC-MS analysis. The GC-MS analysis was performed by using an Agilent GC/MS instrument [Agilent, USA on an Agilent HP-5MS column (30 m, 0.25 mm i.d., 0.25 µm thickness of film, 0.25 µm)] with 5% phenyl methylsiloxane/95% dimethyl olysiloxane. The specific operating conditions were as follows: initial oven temperature was 80 °C held for 2 min, increased to 180 °C at the rate of 10 °C/min held for 7 min, and the final oven temperature was 280 °C at the rate of 30 °C/min, held for 8 min. The helium flow rate was 1.0 mL/min. Splitless injection was used with an ionisation energy of 70 eV. The injector port and detector temperature were 250 °C and 280 °C, respectively. A mass range of 35.00–700.00 m/z at a 150 threshold and 1.562 u/s was applied. Meanwhile, the solvent delay applied was 5 min.

Data processing and statistical analysis. The photosynthetic pigment and stomatal length data were subjected to the Shapiro-Wilk test and an analysis of variance (ANOVA) using Minitab software (version 20.3). Tukey's test at a significance level of 0.05 ($P < 0.05$) was employed to compare the means. For the GC-MS data, the compound identification was compared with the National Institute of Standards and Technology (NIST) mass spectral library (2014). The data matrix, consisting of metabolite names and the peak areas was uploaded to MetaboAnalyst (version 5.0; https://www.metaboanalyst.ca/) for integral normalisation, univariate and multivariate analyses and pathway enrichment analysis.

According to Saccenti et al. (2014), when dealing with a large and complex dataset, multivariate analysis was employed to simplify the data and identify differences between the treatment groups. A Principal Component Analysis (PCA) was used to assess the overall variation and clustering among the samples. A Hierarchical Cluster Analysis

https://doi.org/10.17221/148/2024-PPS

Table 1. Choy sum's significant metabolites ($P < 0.05$) upon *Turnera subulata* LAE application, by the one-way ANOVA through Tukey's test (ESM Table S2)

Significant metabolites ($P < 0.05$)	*F*-value	*P*-value
Gluconic acid, (6TMS)	69.2160	< 0.001
Sucrose, 8TMS derivative	38.7080	< 0.001
L-Sorbopyranose, (1S,2R,3S)-, 5TMS	38.6380	< 0.001
1,1-Ethanediol, diacetate	38.0680	< 0.001
Oxalic acid (2TMS)	33.7670	< 0.001
Erythritol (4TMS)	33.6180	< 0.001
Ethanolamine (3TMS)	33.1050	< 0.001
10-Methylnonadecane	32.8160	< 0.001
Malic acid, 3TMS derivative	30.9460	< 0.001
L-Threonine, 3TMS derivative	30.8840	< 0.001
D-(+)-Turanose, octakis(trimethylsilyl) ether	30.8090	< 0.001
L-Lysine (3TMS)	30.6520	< 0.001
Xylitol, (5TMS)	30.4840	< 0.001
L-threonic acid, tetra-TMS	30.4670	< 0.001
D-Trehalose, 7TMS derivative	30.3470	< 0.001
Galactose MEOX 5TMS-2	30.2490	< 0.001
4-Hydroxyphenylpyruvic acid (3TMS)	30.1210	< 0.001
D-Gluconic acid, 6TMS derivative	30.0370	< 0.001
1,4-Butanediol, bis-TMS	28.0370	< 0.001
4-Pentenoic acid, TMS derivative	26.6610	< 0.001
12-Hydroxyoctadecanoic acid, (2TMS)	26.3940	< 0.001
L-Isoleucine (2TMS)	25.3250	< 0.001
.beta.-D-Galactofuranose, 1,2,3,5,6-pentakis-O-(trimethylsilyl)-	25.0240	< 0.001
L-(+)-Tartaric acid 4(TMS)	24.4110	< 0.001
.alpha.-D-Lactose, (8TMS)	23.3290	< 0.001
Heneicosane	21.6150	< 0.001
Maltose, 8TMS derivative	20.6030	< 0.001
Tyrosine (3TMS)	20.3610	< 0.001
D-Glucitol, 6TMS derivative	19.6600	< 0.001
2-Hydroxyvaleric acid, TMS	19.6520	< 0.001
L(-)-Fucose, tetrakis(trimethylsilyl) ether	16.4500	< 0.001
2-O-Glycerol-.alpha.-d-galacto-pyranoside, hexa-TMS	16.4050	< 0.001
D-Psicofuranose, pentakis(trimethylsilyl) ether	15.1500	< 0.001
Ribonic acid-5TMS	12.2260	< 0.001
Glycine (3TMS)	12.1710	< 0.001
1-Monopalmitin, 2TMS derivative	11.8480	< 0.001
Pyruvic acid (TMS)	11.2070	< 0.001
L-Leucine (2TMS)	10.5800	< 0.001
Arabinose, 4TMS derivative	10.4810	< 0.001
Leu-Gly, N-trimethylsilyl-, trimethylsilyl ester	10.2550	< 0.001
13-Octadecenal, (Z)-	9.9922	< 0.001
.alpha.-D-Arabinopyranose (4TMS)	9.8443	< 0.001
Succinic acid (2TMS)	8.8650	< 0.001
Glycerol (3TMS)	7.1561	< 0.001
L-Proline (2TMS)	6.8092	< 0.001
Glucose-MOX-5TMS-PK1	5.1303	< 0.001
Phosphoric acid TMS	4.0480	< 0.05
Lyxose, tetra-(trimethylsilyl)-ether	3.9170	< 0.05
Erythronic acid, tetrakis-TMS	3.8016	< 0.05

(HCA) and heatmap visualisation were used to illustrate patterns and similarities in the metabolite levels across the different treatments. Furthermore, a metabolic pathway enrichment analysis was performed to identify the key biochemical pathways that were affected by the treatments.

RESULTS

Effect of the *T. subulata* leaf aqueous extract on the photosynthetic pigments and stomata length. The treatments significantly affected the SPAD of the choy sum, as in Figure 1A. In particular, choy sum treated with the 100 mg/mL LAE showed a significant decrease (25%) compared to the control. Similarly, the *chl a* and *chl b* were significantly decreased (Figure 1B) when treated with 100 mg/mL LAE (65% and 71%, respectively). Figure 2A shows a noticeable trend of the stomatal length reduction in a dose-dependent manner. The stomata length decreased by 45% when exposed to the 100 mg/mL treatment. According to Figure 2B, different extract concentrations modified the abaxial (lower) surface. At 100 mg/mL, the stomata were noticeably smaller, thinner, flaccid, and constricted compared to the well-defined, open, elliptical shape in the control.

Analysis of the metabolites in the choy sum. The GC-MS based metabolomics analysis successfully identified 51 metabolites [Electronic Supple-

https://doi.org/10.17221/148/2024-PPS

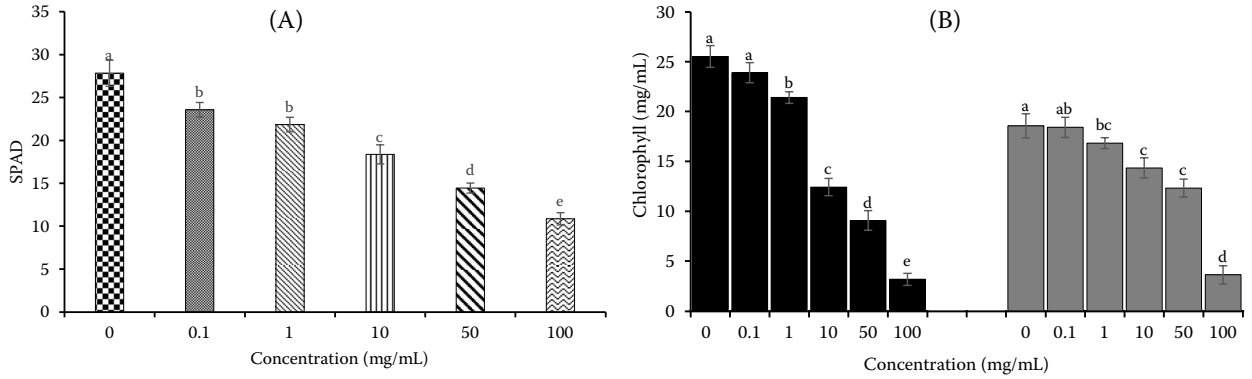

Figure 1. Effect of *Turnera subulata* LAE on the (A) SPAD values and (B) *chl a* and *chl b* of the choy sum
Different letters indicate significant differences according to Tukey's test ($P < 0.05$). Data presented as mean ± standard error from five replicates of sample size ($n = 5$). Bars indicate standard errors of the mean (SEM)

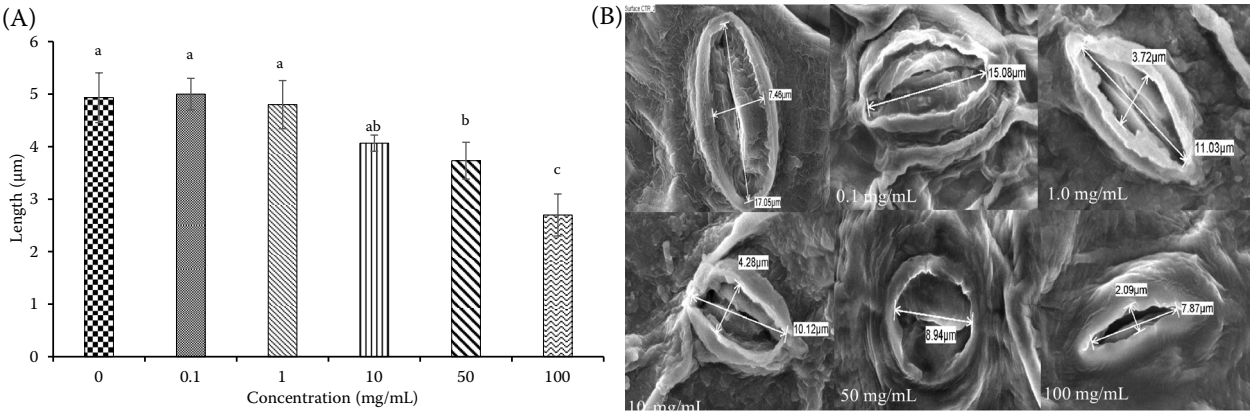

Figure 2. The effect of different concentrations of *Turnera subulata* LAE on (A) the stomata length of choy sum
Different letters on the bar signify significant differences in Tukey's test ($P < 0.05$). The data is expressed as mean ± error with $n = 9$. The standard error is represented by the bars; and (B) Stomatal images captured through SEM at × 3 500 magnification

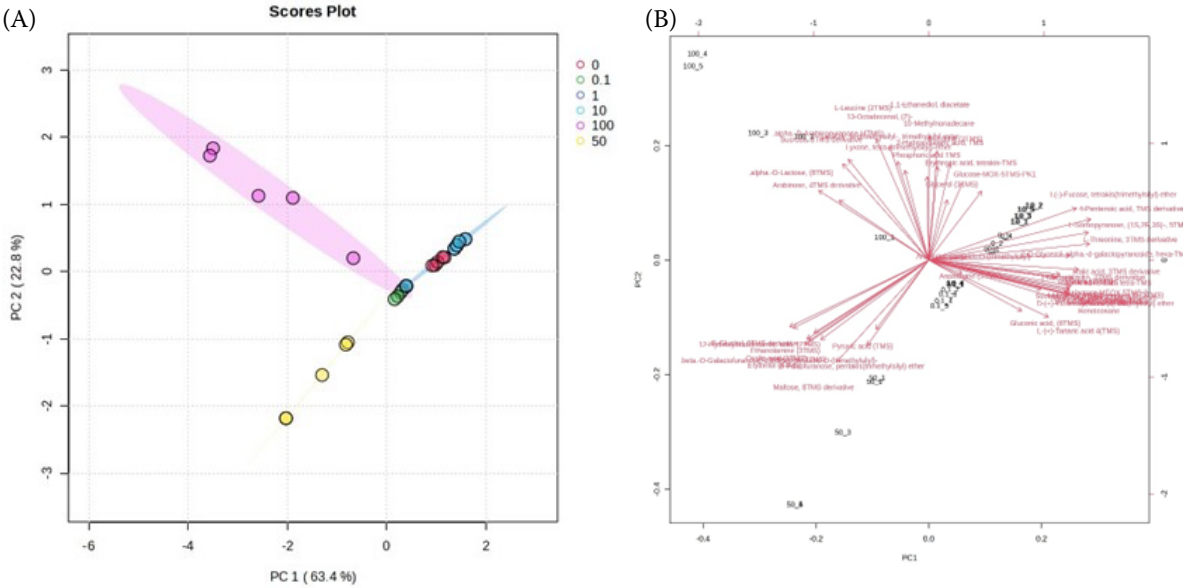

Figure 3. PCA score plot derived from the metabolites of choy sumexposed to the *Turnera subulata* LAE at different concentrations (A) and biplot of metabolites of choy sum upon application of *T. subulata* LAE (B)

https://doi.org/10.17221/148/2024-PPS

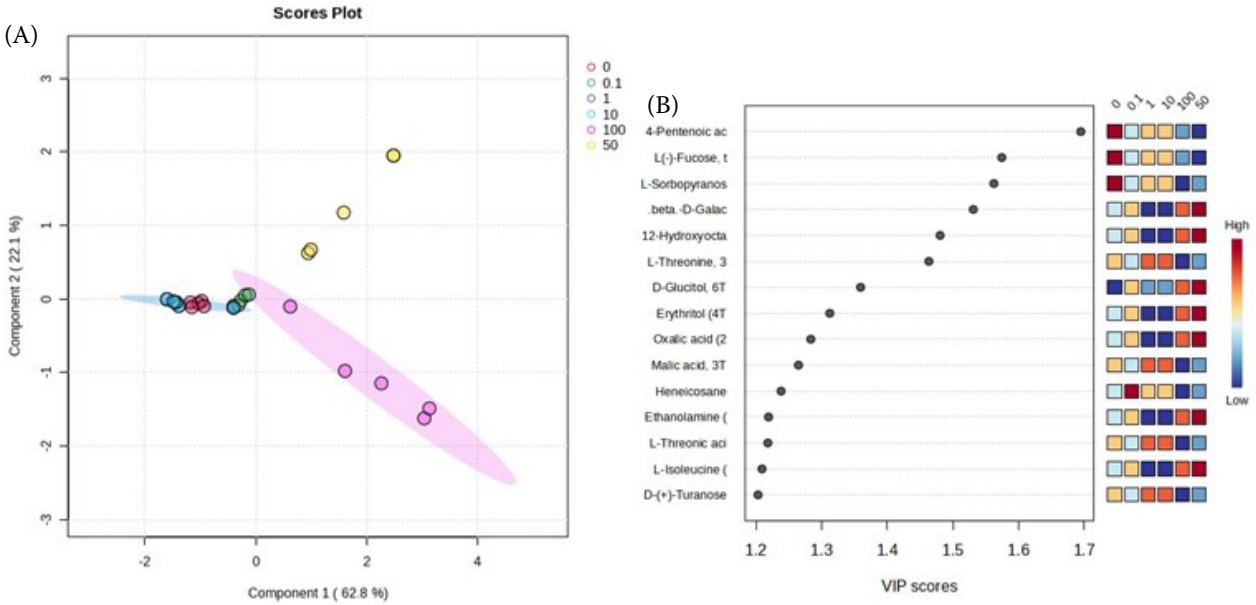

Figure 4. PLS-DA score plot of choy sum exposed to the *Turnera subulata* LAE at different concentrations (A) and VIP from PLS-DA of metabolites ofchoy sum (B)

mentary Material (ESM) Table S1], of which 49 are statistically significant ($P < 0.05$) (Table 1). The unsupervised Principal Component Analysis (PCA) revealed clear separation among the tested concentrations with the first two principal components (PC1 and PC2) achieving a total variation of 86%.

The effect of different *T. subulata* LAE concentrations on the metabolite composition of choy sum was demonstrated by the PCA score plot (Figure 3A). The different *T. subulata* LAE concentrations were divided into three distinct groups. The control (0.0 mg/mL) samples clustered with 0.1, 1.0, and 10.0 mg/mL along PC1 (63.4%), with 0.1 and 1.0 mg/mL samples overlapping considerably. In contrast, 50 and 100 mg/mL treatments were clearly separated from others, with Arabinose, 4TMS and Glucose-MOX-5TMS contributing to the separation of 100 mg/mL according to the biplot (Figure 3B).

Meanwhile, metabolites that were crucial in distinguishing among treatments are highlighted in the Partial Least Squares–Discriminant Analysis (PLS-DA) loading plot (Figure 4A), with those located farther from the centre presenting a significant impact on the PLS-DA. Those with variables important in projection (VIP) VIP > 1 are selected and considered as valuable markers (Beatriz et al. 2014). In Figure 4B, 15 metabolites with VIP > 1 and $P < 0.05$ were identified. Among the metabolites, the 4-Pentenoic acid (VIP = 1.6949) was shown to have the highest VIP, followed by L(-)-Fucose, tetrakis(trimethylsilyl) ether, L-Sorbopyranose, (1S,2R,3S)-, 5TMS, beta.-D-Galactofuranose, 1,2,3,5,6-pentakis-O-(trimethylsilyl)- and 12-Hydroxyoctadecanoic acid, (2TMS). The pathway enrichment analysis was further conducted to identify the biological pathways affected by these 15 metabolites.

Hierarchical clustering analysis (HCA) and heatmap analysis. The HCA classified the metabolites into related groups, with a dendrogram sorting them by similarity patterns (Figure 5). The heat map, using a colour scheme from blue (lowest) to red (highest) to indicate the relative concentrations, showed two distinct clusters among the metabolites affected by the different concentrations of *T. subulata* LAE. The metabolites exhibited different levels, increasing at concentrations ranging from 0.1 to 50.0 mg/mL and decreasing when treated with 100 mg/mL of *T. subulata* LAE. Specifically, carbohydrates, amino acids, and fatty acids were some of the metabolites that decreased at 100 mg/mL, such as 4-pentanoic acid, L(-)-fucose, L-sorbopyranose, L-threonine, malic acid, and heneicosane.

The Kyoto Encyclopedia of Genes and Genomes (KEGG) pathway enrichment analysis was used to identify the metabolic pathways in the choy sum that were affected by the *T. subulata* LAE (Figure 6). The obtained metabolites were assigned to 15 pathways (Figure 6). It was found that the allelopathic effects against choy sum at 100 mg/mL impacted the lipid metabolism (glycerophospholipid me-

https://doi.org/10.17221/148/2024-PPS

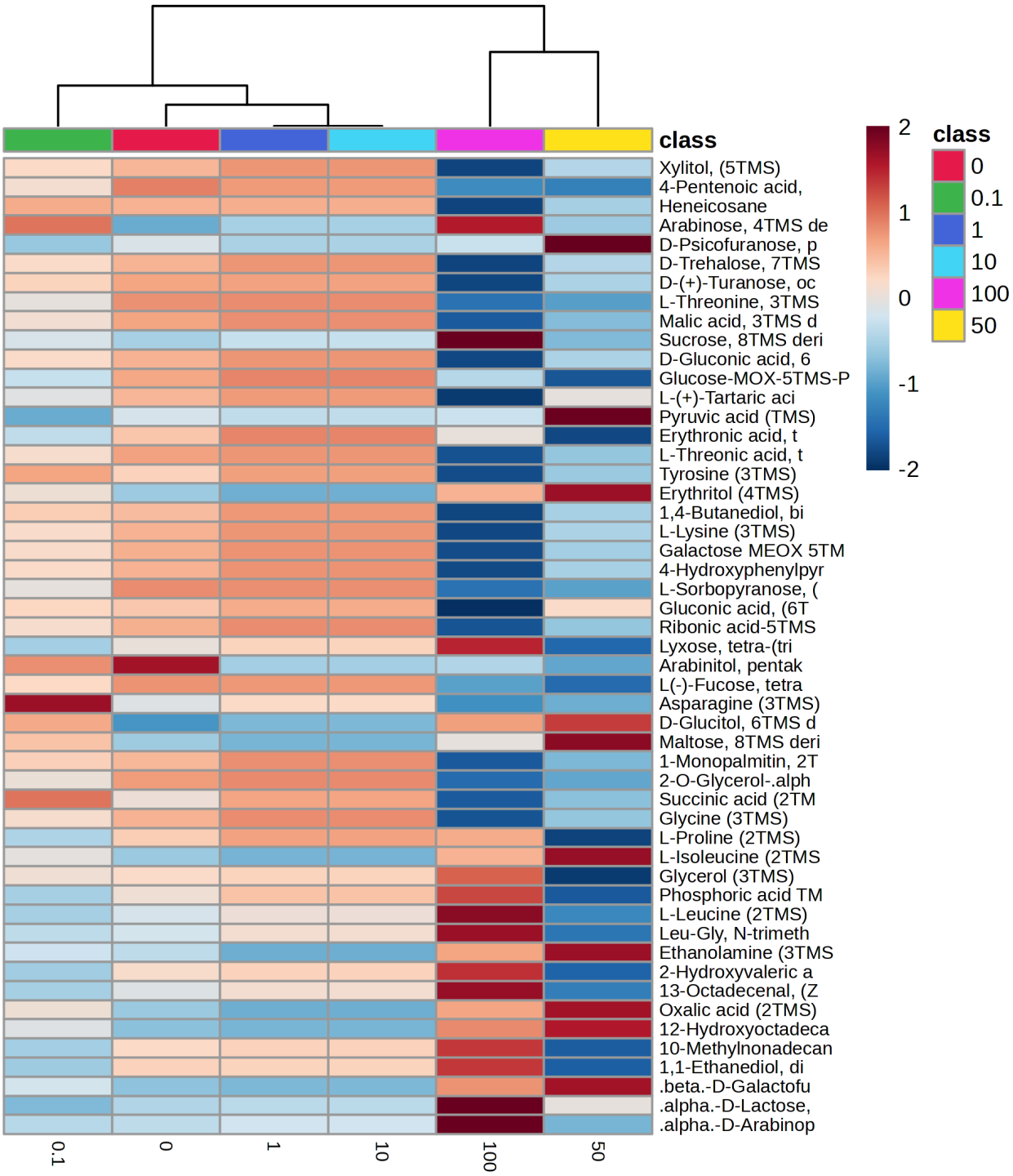

Figure 5. Heat map with a dendrogram of the identified metabolites in the choy sum exposed to the *Turnera subulata* LAE at different concentrations

The row displays metabolites, and the column represents the concentration. The heat map scale ranges from 3.3 to –3.1. Red represents the highest value, and blue represents the lowest value

tabolism) and amino acid metabolism (glycine, serine, and threonine metabolism; valine, leucine, and isoleucine biosynthesis) (Figure 7). Following the result, ethanolamine was altered significantly in the glycerophospholipid metabolism (Figure 7A) due to the association of the phosphatidylcholine and phosphatidylethanolamine biosynthesis. Other pathways that *T. subulata* LAE impacted were iden-

https://doi.org/10.17221/148/2024-PPS

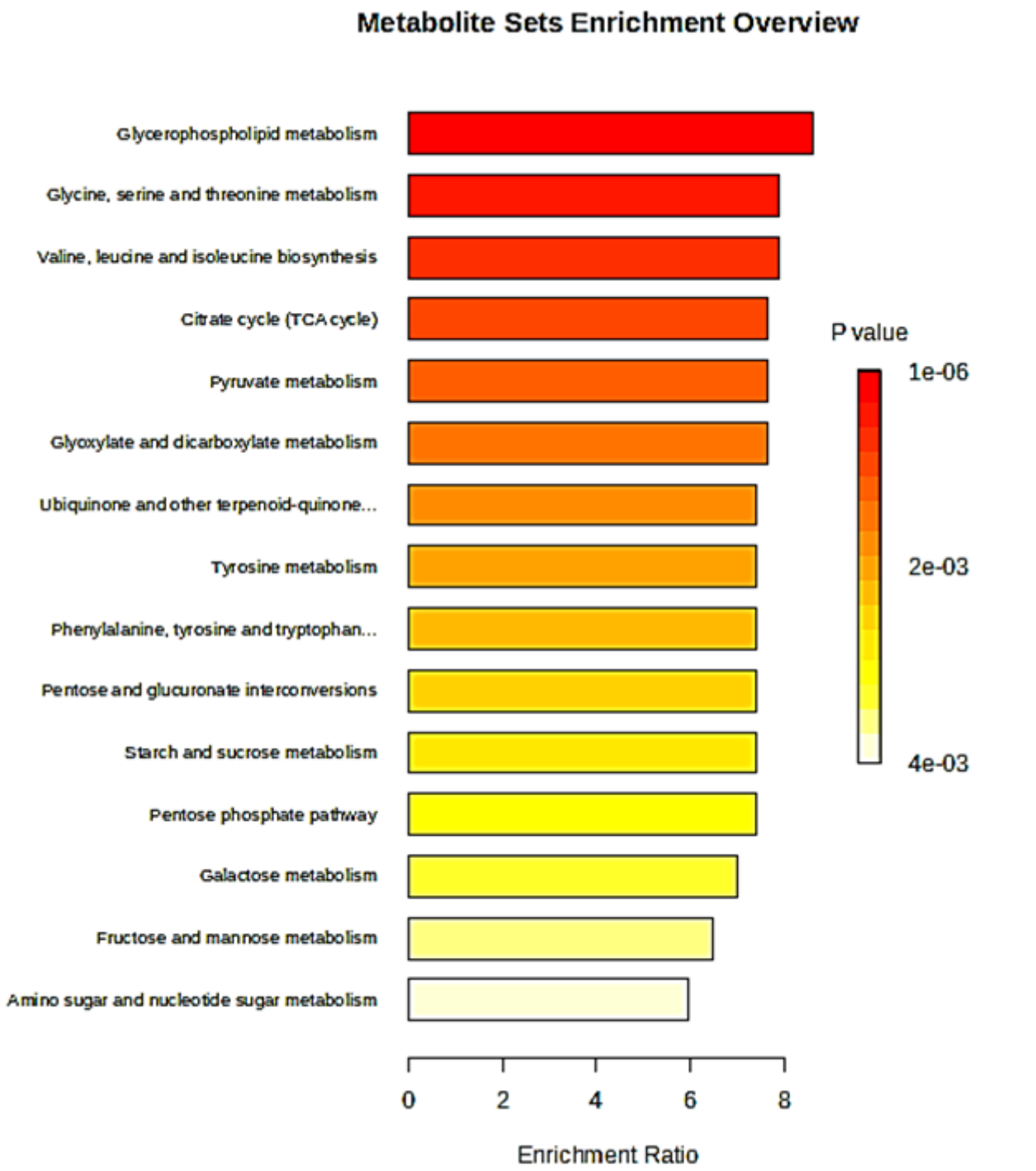

Figure 6. KEGG Pathway enrichment analysis of choy sum when treated with *Turnera subulata* LAE

tified as the amino acid metabolism, namely glycine, serine, and threonine metabolism (Figure 7B), and valine, leucine, and isoleucine biosynthesis. The increase of L-isoleucine, L-leucine, L-proline, and asparagine indicated that choy sum was greatly affected by the *T. subulata* LAE at 100 mg/mL. However, L-threonine seems to decrease at this concentration.

DISCUSSION

The finding suggests that choy sum exposed to *T. subulata* reduced the iron levels, thus decreasing the chlorophyll content to cope with the adverse effect of allelopathy (Figure 1A). This hindered the ability of the plant to photosynthesise efficiently. The reduction in the chlorophyll content is aligned

https://doi.org/10.17221/148/2024-PPS

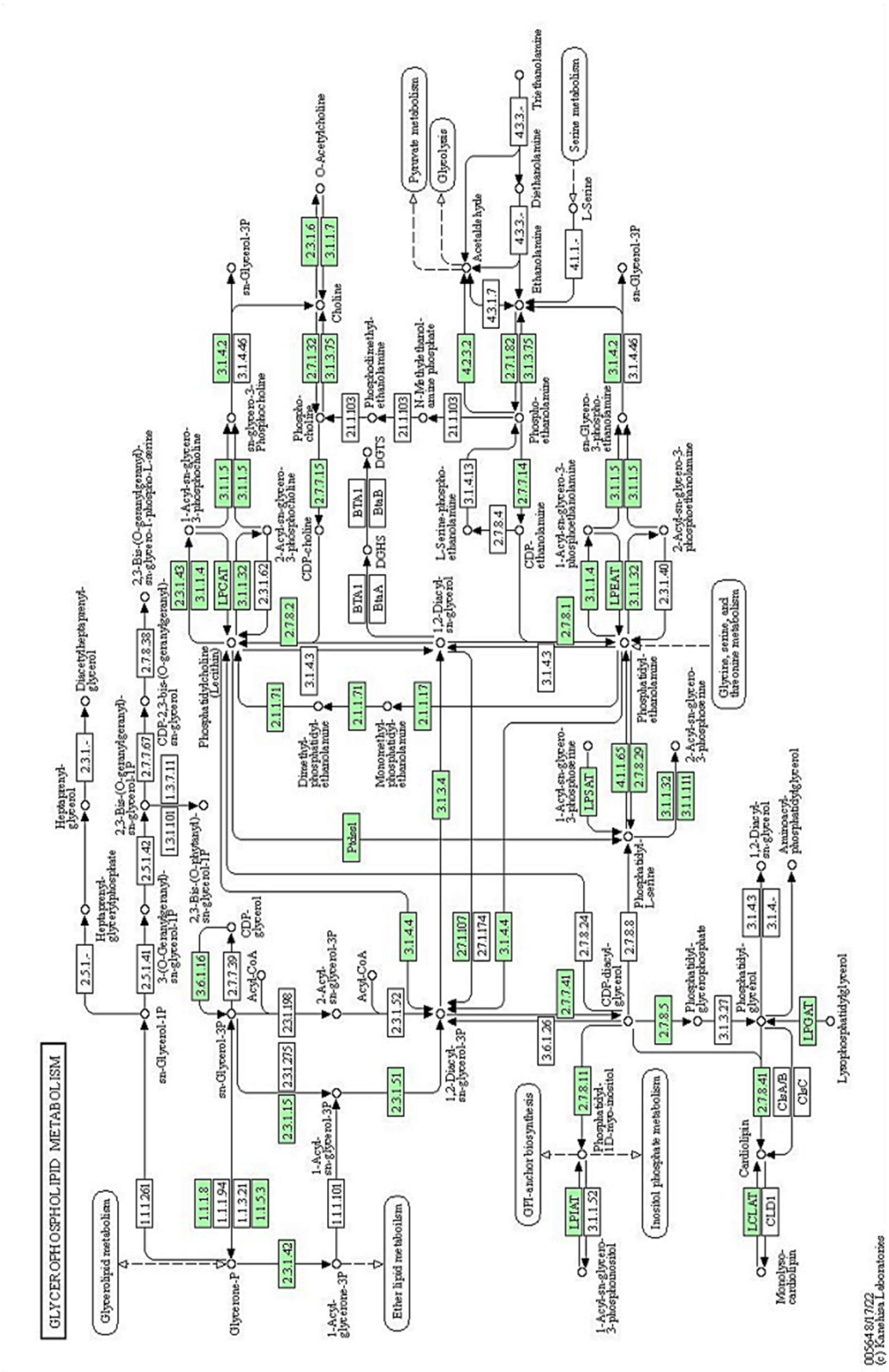

Figure 7A. Metabolism affected in the choy sum, (A) Glycerophospholipid metabolism of choy sum

https://doi.org/10.17221/148/2024-PPS

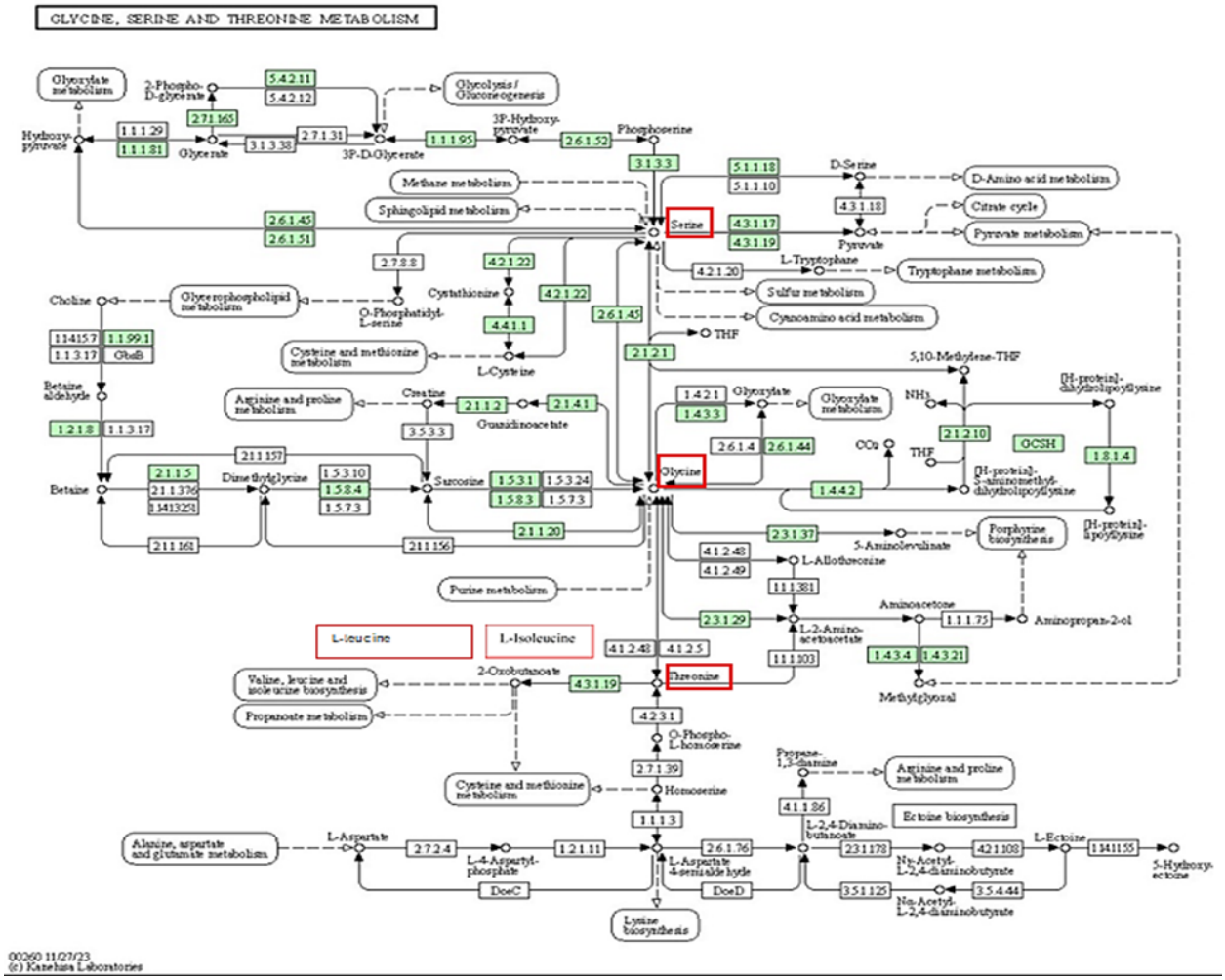

Figure 7B. Metabolism affected in the choy sum, (B) glycine, serine, and threonine metabolism

with a previous study by Ning et al. (2023), who observed that iron chelation by allelochemicals leads to a decrease in the chlorophyll synthesis. Similarly, Wang et al. (2018) observed that *Hippophae rhamnoides* extracts significantly inhibited the chlorophyll content in *Amygdalus pedunculata* seedlings at a concentration of 0.1 g/mL, reducing their ability to absorb and utilise light efficiently. Additionally, the stomatal changes observed in Figure 2A align with Fu et al. (2019), where the application of phenolic acids affected the stomatal opening and reduced the stomatal length and width of *Rhododendron delavayi* leaves. The LAE induced structural changes in the stomata at higher concentrations, making them smaller, thinner, flaccid, and constricted (Figure 2B). This indicates that a high concentration impacts the turgor pressure within the guard cells, causing diverse structural changes in plant tissues (Mushtaq et al. 2019).

The stomatal structure was notably impacted, particularly at elevated concentrations (100 mg/mL). The SEM showed that the stomata became reduced in size, appeared constricted, and exhibited signs of flaccidity. These physical changes indicate a potential disruption in the turgor pressure regulation of guard cells, possibly due to alterations in the osmotic balance or modifications in the cell wall. These observed structural variations are consistent with the research conducted by Fu et al. (2019), which reported stomatal disruption induced by phenolic acids in *Rhododendron delavayi*, as well as the findings by Mushtaq et al. (2019), who noted ultrastructural alterations caused by allelochemicals in *Cassia tora* and *Allium cepa*.

The hierarchical clustering and heatmap analysis uncovered clear grouping trends, showing that metabolite profiles are regulated differently depending on the concentration of LAE. Lower concentrations

https://doi.org/10.17221/148/2024-PPS

(0.1–10.0 mg/mL) resulted in moderate alterations, while higher concentrations (50–100 mg/mL) led to notable decreases, particularly in sugars and fatty acids. The reduction in beta-D-galactofuranose, alpha-D-lactose, L-threonine, and malic acid indicates a suppression of energy metabolism and biosynthetic activity (Raval et al. 2018; Sun et al. 2019; Gong et al. 2021).

Conversely, downregulated metabolites, such as xylitol, trehalose, and essential amino acids, like L-threonine, tyrosine, and lysine, suggest the potential inhibition of the protein synthesis or the increased catabolism for energy. The decrease in trehalose may indicate weak stress resistance because it helps protect plants from oxidative stress (Nawaz et al. 2022; Al Hinai et al. 2025). Key metabolites for the separation include sugars and sugar alcohols like arabinose, glucitol, and maltose, which were significantly elevated in high-dose treatments. These metabolites help with the osmotic balance and carbohydrate metabolism, suggesting an adaptive response or a shift toward energy storage during stress.

Additionally, increased ethanolamine and phosphoric acid levels in higher treatments indicate membrane lipid turnover and cellular remodelling, common markers of physiological stress or senescence (Li et al. 2022). These metabolic changes reflect that the plant tries to adapt to or counteract treatment damage. Membrane lipid turnover is a continuous process that involves the breakdown and creation of membrane lipids within plant cells (Yu et al. 2021). This process is important for maintaining the integrity, fluidity, and function of membranes, especially when the plants face stress (Guo et al. 2019; Liu et al. 2019). When the choy sum was exposed to allelochemicals found in the aqueous extract of *T. subulata* LAE, the cell membranes were damaged or destabilised. In response, choy sum initiates lipid turnover to remove damaged lipids and produce new ones. The increase in ethanolamine and phosphoric acid observed at higher concentrations of LAE suggests that there is enhanced phospholipid metabolism. Both compounds are essential intermediates in the synthesis and breakdown of phosphatidylethanolamine and other membrane phospholipids. This finding indicated that LAE may be triggering oxidative or chemical stress, which affects the cell membranes. As a result, the plants may attempt to adjust their membranes to cope with this stress. Such reactions are often linked to early signs of ageing or cell damage, highlighting that high levels of LAE can induce considerable physiological stress in choy sum. The clustering pattern highlights that metabolite profiles in the 50 and 100 treatment groups differ significantly from the untreated or lightly treated controls. These results aligned with the studies by Bruno et al. (2025), Hasanuzzaman et al. (2018) and Zhu et al. (2021), showing that allelochemicals caused stress that often-altered carbohydrate metabolism, amino acid, and lipid-derived metabolites in plants.

To clarify the MOA of *T. subulata*, the study implemented untargeted metabolomics using GC-MS, uncovering significant changes in the primary metabolism within choy sum, particularly in the lipid, amino acid, and carbohydrate pathways. Out of 51 metabolites identified, 49 were found to be significant ($P < 0.05$), with 15 having VIP scores over 1, identifying them as key biomarkers of LAE. Notably, 4-pentenoic acid, L(-)-fucose, and L-sorbopyranose exhibited marked treatment-dependent decreases, while the levels of L-leucine, L-isoleucine, L-proline, and asparagine increased. These trends suggest the reprogramming of the energy and nitrogen metabolism induced by stress. Ethanolamine, a metabolite that showed significant changes in treated plants, is essential in glycerophospholipid metabolism. This alteration indicates the potential destabilisation of membranes, as ethanolamine serves as a precursor to phosphatidylethanolamine, a major phospholipid in plant membranes. Sharma et al. (2023) pointed out that the remodelling of membrane lipids is a typical response to abiotic stress, highlighting its signalling role and impact on membrane fluidity. Therefore, the reduction in ethanolamine levels indicates a possible breakdown of cellular membranes, which may be a mechanism of action for *T. subulata*.

In reaction to stress, the choy sum accumulated beneficial amino acids like L-proline, L-isoleucine, and asparagine. These metabolites act as antioxidants, osmolytes, and pH regulators, helping to reduce oxidative damage and sustain cellular balance (Khan et al. 2020; Ingrisano et al. 2023). This accumulation suggests that a compensatory metabolic mechanism has been activated to alleviate the stress caused by LAE.

The *T. subulata* LAE significantly impacted the metabolism of choy sum, as shown by the KEGG pathway enrichment analysis (Figure 6). Specifi-

https://doi.org/10.17221/148/2024-PPS

cally, the LAE disrupted lipid metabolism, particularly the production of glycerophospholipids (Figure 7A), essential components of cell membranes. Lipids work as signal mediators in plant cells, lowering stress responses and triggering defence mechanisms in response to drought, osmotic, and salt stress (Sharma et al. 2023). Additionally, the amino acid metabolism was affected, with changes in the pathways related to glycine, serine, threonine, valine, leucine, and isoleucine (Figure 7B). The decline in ethanolamine, a key precursor for membrane lipids, further supports the disruption of cell membrane structure. The accumulation of proline, asparagine, leucine, and isoleucine in plants is in response to osmotic stress and the subsequent recovery of plants (Liu & Lin 2020; Ingrisano et al. 2023). To counteract these metabolic disturbances, the plant accumulated amino acids such as proline, asparagine, leucine, and isoleucine (Figure 7B). These compounds play a protective role, helping the plant withstand stress by acting as antioxidants and maintaining the cellular balance. The fluctuation of these amino acids is a sign of plant stress tolerance by detoxifying reactive oxygen species, regulating the pH, and osmotic adjustments (Khan et al. 2020). These findings suggest that the choy sum plant activated specific metabolic responses to mitigate the harmful effects of the *T. subulata* LAE.

CONCLUSION

T. subulata LAE exerted significant allelopathic effects against choy sum, affecting the SPAD, chlorophyll content, and stomata length. Multivariate analyses of PCA and PLS-DA indicated that choy sum exhibited distinct responses to LAE. An increase in the metabolite levels of amino acids and fatty acids suggested the defence mechanisms of choy sum against *T. subulata* LAE, while a decrease in several metabolites indicated the susceptibility of choy sum against *T. subulata* LAE. To sum up, *T. subulata* is a potential allelopathic species that could hinder the growth of neighbouring plant species by altering important metabolic pathways. This study marks the first step in understanding the phytotoxic mechanisms of *T. subulata* LAE on target plants.

Acknowledgement: This research was supported by the Research Grant No. FRGS/1/2019/WAB01/UNISZA/03/2 from the Ministry of Higher Education, Malaysia. The authors wish to express their gratitude to Mr. Faris Ilyamuddin bin Hamzah for his assistance in handling the GC-MS instrument.

REFERENCES

Al Hinai M.S., Rehman A., Siddique K.H., Farooq M. (2025): The role of trehalose in improving drought tolerance in wheat, Journal of Agronomy and Crop Science, 211: e70053.

Andrade-Pinheiro J.C., Sobral de Souza C.E., Ribeiro D.A., Silva A.D.A., da Silva V.B., dos Santos A.T.L., Juno Alencar Fonseca V., de Macêdo D.G., et al. (2023): LC-MS analysis and antifungal activity of *Turnera subulate* Sm. Plants, 12: 415.

Anzano A., Bonanomi G., Mazzoleni S., Lanzotti V. (2022): Plant metabolomics in biotic and abiotic stress: a critical overview. Phytochemistry Reviews, 21: 503–524.

Beatriz G.-P., Lennart E., Johan T. (2014): Variable influence on projection (VIP) for orthogonal projections to latent structures (OPLS). Journal of Chemometrics, 28: 623–632.

Brito Filho S.G.D., Fernandes M.G., Chaves O.S., Chaves M.C.D.O., Araruna F.B., Eiras C., Leite J.R.D.S.D.A., Agra M.D.F., et al. (2014): Chemical constituents isolated from *Turnera subulata* Sm. and electrochemical characterization of phaeophytin b. Química Nova, 37: 603–609

Bruno L., Mircea D.M., Araniti F. (2025): Metabolomic insights into the allelopathic effects of *Ailanthus altissima* (Mill.) swingle volatile organic compounds on the germination process of *Bidens pilosa* (L.). Metabolites, 15: 12.

Chai T.T., Wong F.C. (2012): Whole-plant profiling of total phenolic and flavonoid. Journal of Medicinal Plants Research, 6: 1730–1735.

de Almeida L., Gaspar Y.M.D.S., Silva A.A.R., Porcari A.M., Lacerda J.J.D.J., Araújo F.D.D.S. (2024): Allelopathic effect and putative herbicidal allelochemicals from *Jatropha gossypiifolia* on the weed *Bidens bipinnata*. Acta Physiologiae Plantarum, 46: 61.

Fu Y.H., Quan W.X., Li C.C., Qian C.Y., Tang F.H., Chen, X.J. (2019): Allelopathic effects of phenolic acids on seedling growth and photosynthesis in *Rhododendron delavayi* Franch. Photosynthetica, 57: 377–387.

Gong Y., Song J., Palmer L.C., Vinqvist-Tymchuk M., Fillmore S., Toivonen P., Zhang, Z. (2021): Tracking the development of the superficial scald disorder and effects of treatments with diphenylamine and 1-MCP using an untargeted metabolomic approach in apple fruit. Food Chemistry: Molecular Sciences, 2: 100022.

Gowtham H.G., Hariprasad P., Singh S.B., Niranjana S.R. (2016): Biological control of Phomopsis leaf blight of brinjal (*Solanum melongena* L.) with combining phylloplane

https://doi.org/10.17221/148/2024-PPS

and rhizosphere colonising beneficial bacteria. Biological Control, 101:123–129.

Guo Q., Liu L., Barkla B.J. (2019): Membrane lipid remodeling in response to salinity. International Journal of Molecular Sciences, 20: 4264.

Hasanuzzaman M., Mahmud J.A., Anee T.I., Nahar K., Islam M.T. (2018): Drought stress tolerance in wheat: Omics approaches in understanding and enhancing antioxidant defense. In: Zargar M.S., Zargar M.Y. (eds): Abiotic Stress-Mediated Sensing and Signaling in Plants: An Omics Perspective. Singapore, Springer: 267–307.

Henning P.M., Roalson E.H., Mir W., McCubbin A.G., Shore J.S. (2023): Annotation of the *Turnera subulata* (Passifloraceae) draft genome reveals the S-Locus evolved after the divergence of Turneroideae from Passifloroideae in a stepwise manner. Plants, 12: 286.

Huang X., Zhu Y., Su W., Song S., Chen R. (2024): Widely-targeted metabolomics and transcriptomics identify metabolites associated with flowering regulation of Choy Sum. Scientific Report, 14: 10682.

Ingrisano R., Tosato E., Trost P., Gurrieri L., Sparla F. (2023): Proline, cysteine and branched-chain amino acids in abiotic stress response of land plants and microalgae. Plants (Basel), 12: 3410.

Jahangir M., Abdel-Farid I.B., Kim H.K., Choi Y.H., Verpoorte R. (2009): Healthy and unhealthy plants: The effect of stress on the metabolism of *Brassicaceae*. Environmental and Experimental Botany, 67: 23–33.

Katiyar P., Pandey N., Keshavkant S. (2022): Gamma radiation: A potential tool for abiotic stress mitigation and management of agroecosystem. Plant Stress, 5: 100089.

Khan N., Ali S., Zandi P., Mehmood A., Ullah S., Ikram M., Ismail M.A.S., Babar M.A. (2020): Role of sugars, amino acids and organic acids in improving plant abiotic stress tolerance. Pakistan Journal of Botany, 52: 355–363.

Li Z., Cheng B., Zhao Y., Luo L., Zhang Y., Feng G., Han L., Peng Y., et al. (2022): Metabolic regulation and lipidomic remodelling in relation to spermidine-induced stress tolerance to high temperature in plants. International Journal of Molecular Sciences, 23: 12247.

Liu L., Lin L. (2020): Effect of heat stress on *Sargassum fusiforme* leaf metabolome. Journal of Plant Biology, 63: 229–241.

Liu X., Ma D., Zhang Z., Wang S., Du S., Deng X., Yin L. (2019): Plant lipid remodeling in response to abiotic stresses. Environmental and Experimental Botany, 165: 174–184.

Lichtenthaler H.K., Wellburn A.R. (1983): Determinations of total carotenoids and chlorophylls *a* and *b* of leaf extracts in different solvents. Biochemical Society Transaction, 11: 591–592.

Luz J.R.D.D., Barbosa E.A., Nascimento T.E.S.D., Rezende A.A.D., Ururahy M.A.G., Brito A.D.S., Araujo-Silva G., López J.A., et al. (2022): Chemical characterization of flowers and leaf extracts obtained from *Turnera subulata* and their immunomodulatory effect on LPS-Activated RAW 264.7 macrophages. Molecules, 27: 1084.

Mashabela M.D., Masamba P., Kappo A.P. (2023). Applications of metabolomics for the elucidation of abiotic stress tolerance in plants: A special focus on osmotic stress and heavy metal toxicity. Plants, 12: 269

Mushtaq W., Ain Q., Siddiqui M.B., Hakeem K.R. (2019). Cytotoxic allelochemicals induce ultrastructural modifications in *Cassia tora* L. and mitotic changes in *Allium cepa* L.: A weed versus weed allelopathy approach. Protoplasma, 256: 857–871.

Nawaz M., Hassan M.U., Chattha M.U., Mahmood A., Shah A.N., Hashem M., Qari S.H. (2022): Trehalose: A promising osmo-protectant against salinity stress – physiological and molecular mechanisms and future prospective. Molecular Biology Reports, 49: 11255–11271.

Ning X., Lin M., Huang G., Mao J., Gao Z., Wang X. (2023): Research progress on iron absorption, transport, and molecular regulation strategy in plants. Frontiers in Plant Science, 14: 1190768.

Oshunsanya S.O., Nwosu N.J., Li Y. (2019): Abiotic stress in agricultural crops under climatic conditions. In: Sustainable Agriculture, Forest and Environmental Management, Singapore, Springer: 71–100.

Raval S.S., Mahatma M.K., Chakraborty K., Bishi S.K., Singh A.L., Rathod K.J., Jadav J.K., Sanghani J.M., Mandavia M.K., Gajera H.P., Golakiya B.A. (2018): Metabolomics of groundnut (*Arachis hypogaea* L.) genotypes under varying temperature regimes. Plant Growth Regulator, 84: 493–505.

Saccenti E., Hoefsloot H.C.J., Smilde A.K., Westerhuis J.A., Hendriks M.M.W.B. (2014): Reflections on univariate and multivariate analysis of metabolomics data. Metabolomics, 10: 361–374.

Sahrir M.A.S., Yusoff N., Azizan K.A., Aridi N.A.M. (2024): Assessing the allelopathic effect of *Chrysopogon zizanioides* (L.) Roberty root methanolic extract on *Brassica rapa* subsp. *chinensis* var. *parachinensis* using an untargeted metabolomic approach. Chilean Journal of Agricultural Research, 84: 154–165.

Saravanan M., Senthilkumar P., Chinnadurai V., Murugesan Sakthivel K., Rajeshkumar R., Pugazhendhi A. (2020): Antiangiogenic, anti-inflammatory and their antioxidant activities of *Turnera subulata* Sm. (Turneraceae). Process Biochemistry, 89: 71–80.

Saravanan M., Senthilkumar P., Kalimuthu K., Chinnadurai V., Vasantharaj S., Pugazhendhi A. (2018). Phytochemical and pharmacological profiling of *Turnera subulata* Sm., a vital medicinal herb. Industrial Crops and Products, 124: 822–833.

https://doi.org/10.17221/148/2024-PPS

Sharma P., Goyal A., Ahlawat Y.K., Lakra N., Zaid A., Siddique K.H. (2023). Drought and heat stress mediated activation of lipid signaling in plants: a critical review. Frontiers in Plant Science, 14: 1216835.

Sun X., Han G., Meng Z., Lin L., Sui N. (2019): Roles of malic enzymes in plant development and stress responses. Plant Signaling and Behavior, 14.

Szewczyk K., Bogucka-Kocka A., Vorobets N., Grzywa-Celińska A., Granica, S. (2020): Phenolic composition of the leaves of *Pyrola rotundifolia* L. and their antioxidant and cytotoxic activity. Molecules, 25: 1749.

Tashim D.N.N.A.Z., Md P., Sukri R.S., Jaafar S.M., Metali F. (2021): Allelopathic effects of *Mangifera indica* leaves on the growth performance of *Brassica rapa* '*Chinensis*' (Pak choi). Research on Crops, 22: 564–575.

Wang X., Wang J., Zhang R., Huang Y., Feng S., Ma X., Zhang Y., Sikdar A., et al. (2018): Allelopathic effects of aqueous leaf extracts from four shrub species on seed germination and initial growth of *Amygdalus pedunculata* Pall. Forests, 9: 711.

Wishart D.S., Cheng L.L., Copié V., Edison A.S., Eghbalnia H.R., Hoch J.C. (2022): NMR and metabolomics – A roadmap for the future. Metabolites, 12: 678.

Xiao X., Ma Z., Zhou K., Niu Q., Luo Q., Yang X., Chu X., Shan G. (2025): Elucidating the underlying allelopathy effects of *Euphorbia jolkinii* on *Arundinella hookeri* using metabolomics profiling. Plants, 14: 123.

Yaakob N., Yusoff N., Azizan K.A., Azemin A., Mahmud K., Che Lah M.K. (2020): Assessment on allelopathic activity and potential allelochemicals of *Turnera subulata* Sm. Bioscience Research, 15: 123–145.

Yu L., Zhou C., Fan J., Shanklin J., Xu C. (2021): Mechanisms and functions of membrane lipid remodeling in plants. The Plant Journal, 107: 37–53.

Zhu X., Yi Y., Huang L., Zhang C., Shao H. (2021).: Metabolomics reveals the allelopathic potential of the invasive plant *Eupatorium adenophorum*. Plants, 10: 1473.

Zou L., Tan W.K., Du Y., Lee H.W., Liang X., Lei J., Striegel L., Weber N., et al. (2021): Nutritional metabolites in *Brassica rapa* subsp. *chinensis* var. *parachinensis* (choy sum) at three different growth stages: Microgreen, seedling and adult plant. Food Chemistry, 357: 129535.

Received: August 27, 2024
Accepted: May 9. 2025
Published online: December 4, 2025